# Magnetoresistance of Planar Heterostructures Approached on a Theoretical Basis

Stanisław Olszewski and Tomasz Roliński
Institute of Physical Chemistry, Polish Academy of Sciences, Kasprzaka 44/52, 01-224 Warsaw, Poland

Reprint requests to S. O.; E-mail: olsz@ichf.edu.pl

Z. Naturforsch. **67a,** 50 – 56 (2012) / DOI: 10.5560/ZNA.2011-0052
Received July 11, 2011 / revised September 14, 2011

The change of magnetoresistance in dependence on the strength of the magnetic induction is examined theoretically for several heterostructures taken as examples. Different temperatures of the examined samples, concentrations of the electron or hole carriers, and band structure properties are then involved. A general result is that a linear increase of magnetoresistance as a function of the magnetic induction should be obtained for all samples. This finds its counterpart in the behaviour of the experimental data. The ratios of the theoretical slopes of increase to the experimental ones range between 0.1 and 11, but the average ratio amounts to less than 1.8.

*Key words:* Two-Dimensional Interface Heterostructures; Diagonal and Hall Magnetoresistance.
*PACS numbers:* 72.20 My; 73.40 Kp; 73.40 Lq; 73.50 Jt

## 1. Experimental Background and Basic Formulae

A typical experimental behaviour of magnetoresistance $\rho$ of planar crystalline structures is mainly represented by two lines, that of $\rho_{xy}$ and that of $\rho_{xx}$, plotted versus the strength of the magnetic field induction $B$ [1, 2]. The field $B$ is directed normally to the planar crystalline surfaces, say in direction $z$, and $\rho_{xy}$ and $\rho_{xx}$ increase rather systematically with the increase of $B$. If the quantum effects causing the line oscillations can be neglected, and this kind of oscillation damping is connected, especially for $\rho_{xx}$, with not very low temperatures, both lines attain a straightlinear character; nevertheless, they can differ strongly in their slopes. For the most part of cases examined experimentally, the slope of $\rho_{xy}$ is larger than that of $\rho_{xx}$ [1].

A characteristic point concerning the magnetic field dependence of the transport coefficients in metals is that the often cited semiclassical theory of Lifshitz, Azbel, and Kaganov [3] makes predictions which systematically are not confirmed by experiment [4 – 6]. This difficulty can be avoided if the magnetotransport theory is based on two independent relaxation times referring separately to the action of the electric and magnetic field [7]. A list of the theoretical results obtained in this way for the transversal magnetoresistance in three-dimensional metals is compared with the experimental data in [7].

The aim of the present paper is to apply the theory of [7] to the magnetoresistance effects in the planar two-dimensional structures, especially to the problem of the dependencies of $\rho_{xy}$ and $\rho_{xx}$ on $B$. It seems that the functions of $B$ of the diagonal $\rho_{xx}$ were never approached numerically before. In the present paper we do such calculations for 27 planar heterostructures, and the obtained theoretical data are compared with the experiment. In the first step, it can be shown, by neglecting the quantum effects of magnetoresistance, that in fact a linear behaviour of both functions $\rho_{xy}$ and $\rho_{xx}$ in dependence on $B$ should be obtained. In the next step, in course of more accurate calculations, the slopes of these dependencies can be estimated.

An appropriate tensor for the magnetoresistance should be combined of two tensors [7]: one of them is due to the action of the electric field alone and the other tensor is an effect of the presence of the magnetic field. Consequently, the relaxation times entering each of these two tensors are different: one $\tau = \tau_{\mathrm{el}}$ represents solely the effect of the electric field, and the other $\tau = \tau(B)$ is provided by the magnetic field. When both tensors are combined into one tensor, in the diagonal terms of this effective tensor the reciprocal values of $\tau_{\mathrm{el}}$ and $\tau(B)$ add together according to the Matthiessen rule:

$$\frac{1}{\tau_{\mathrm{eff}}} = \frac{1}{\tau_{\mathrm{el}}} + \frac{1}{\tau(B)}. \qquad (1)$$

A characteristic point is that $\tau_{el}$ is independent of the strength of the electric field, but $\tau(B)$ is strongly dependent on $B$. For a planar structure located in the $x,y$-plane, and the magnetic field directed along the $z$-axis, the effective tensor takes the form [7, 8]:

$$\|\rho^{\text{eff}}\| = \frac{m}{n_s e^2 \tau_{\text{el}}} \begin{pmatrix} 1 & 0 \\ 0 & 1 \end{pmatrix} + \frac{m}{n_s e^2 \tau(B)} \begin{pmatrix} 1 & -\xi \\ \xi & 1 \end{pmatrix}. \quad (2)$$

Here $n_s$ is the concentration of the electron carriers in a crystal plane,

$$\xi = \tau(B)\Omega_0, \quad (3)$$

and

$$\Omega_0 = \frac{eB}{mc} \quad (4)$$

is the circular frequency of the electron gyration upon the action of the magnetic field.

It is convenient to represent (2) in the form:

$$\|\rho^{\text{eff}}\| = \|\rho\| + \|\Delta\rho\|. \quad (2a)$$

A characteristic point is that the non-diagonal components of the second tensor in (2) enter unchanged the tensor $\|\rho^{\text{eff}}\|$, so

$$|\rho_{xy}^{\text{eff}}| = |\Delta\rho_{xy}| = \frac{m\xi}{n_s e^2 \tau(B)}. \quad (5)$$

Another characteristic point is that at $B = 0$ the component tensor $\|\Delta\rho\|$ in (2a) vanishes because

$$\frac{1}{\tau(B)} = \frac{\Omega_0}{\xi} = 0. \quad (3a)$$

A result obtained before [7] was that $\xi$ is a constant number independent of the field strength $B$. Therefore, because of (3) and (4), $\tau(B)$ should be inversely proportional to $B$. Evidently, because of (5), this gives a proportionality relation

$$\rho_{xy}^{\text{eff}} \sim B \quad (6)$$

which is a well-established experimental fact known as the Hall effect in three-dimensional structures, but in the planar structures, too.

If we neglect the kinks on the experimental plots of $\rho_{xy}^{\text{eff}}$ due to the quantum effects, the behaviour of (5) versus $B$ is in practice strictly straight-linear. By expressing the resistance in $h/e^2$ units, each unit corresponding to $25.8 \cdot 10^3\ \Omega$, we obtain the slope equal to

$$\frac{|\rho_{xy}^{\text{eff}}|}{B} = \frac{m}{n_s h}\, 17.6 \cdot 10^6 \cdot 25.8 \cdot 10^3, \quad (7)$$

on condition $|\rho_{xy}^{\text{eff}}|$ is expressed in Ohm and $B$ in Gauss; c.g.s. units are next applied for $m$, $n_s$, and $h$. The first number on the right of (7) represents the electron gyration frequency (expressed in radians) due to the field intensity of $B = 1$ G:

$$\Omega_0^{(1\text{ G})} = 17.6 \cdot 10^6\ \text{s}^{-1}. \quad (8)$$

A remarkable agreement of the theoretical results based on (7) with the experimental data for the planar structures has been demonstrated before; see Table 5 in [9]. Supplementary data are calculated in Table 1 of the present paper where the theoretical slope (7) is compared with the experimental one for twelve crystalline compounds [2, 10 – 18] neglected in [9].

An interesting property is represented by the ratio

$$\frac{|\rho_{xy}^{\text{eff}}|}{|\rho_{xx}^{\text{eff}}|} = \frac{\xi[\tau(B)]^{-1}}{\frac{1}{\tau_{\text{el}}} + \frac{1}{\tau(B)}} = \frac{\xi}{\frac{\tau(B)}{\tau_{\text{el}}} + 1} = \frac{\xi}{\frac{\xi}{\Omega_0 \tau_{\text{el}}} + 1} \underset{B\to\infty}{\to} \xi. \quad (9)$$

Table 1. Theoretical slopes of $|\rho_{xy}|$ lines versus $B$ compared with similar slopes obtained from the experimental data; $\rho_{xy}$ are expressed in Ohm and $B$ in Gauss.

| Reference number | $n_s$ in cm$^{-2}$ | Theoretical $\lvert\rho_{xy}^{\text{eff}}\rvert/B$ [see (7)] | Experimental slope $\lvert\rho_{xy}^{\text{eff}}\rvert/B$ |
|---|---|---|---|
| [2] | $1.21 \cdot 10^{11}$ | 0.50 | 0.52 |
| [11] | $1.53 \cdot 10^{11}$ | 0.41 | 0.39 |
| [12] | $1.74 \cdot 10^{11}$ | 0.36 | 0.36 |
| [13][a] | $1.93 \cdot 10^{11}$ | 0.32 | 0.32 |
| [10] | $1.93 \cdot 10^{11}$ | 0.32 | 0.32 |
| [13][b] | $2.18 \cdot 10^{11}$ | 0.29 | 0.29 |
| [14] | $2.37 \cdot 10^{11}$ | 0.26 | 0.26 |
| [15] | $2.65 \cdot 10^{11}$ | 0.24 | 0.21 |
| [13][c] | $2.90 \cdot 10^{11}$ | 0.22 | 0.22 |
| [16] | $3.63 \cdot 10^{11}$ | 0.17 | 0.10 |
| [17] | $3.70 \cdot 10^{11}$ | 0.17 | 0.16 |
| [18] | $5.90 \cdot 10^{11}$ | 0.10 | 0.10 |

[a] see Figure 1 in [13]
[b] see Figure 2 in [13]
[c] see Figure 4 in [13], upper part

This result is obtained because for very large $B$, and for $\xi$ as well as $\tau_{el}$ equal to constant numbers, the ratio

$$\frac{\xi}{\Omega_0 \tau_{el}} \to 0 \tag{10}$$

makes the result of (9) equal to a constant $\xi$. In fact, for very large $B$, the ratio of experimental slopes of $\rho_{xy}^{eff}$ and $\rho_{xx}^{eff}$ tends – in numerous cases of crystal heterostructures – to a constant number. A quantum-mechanical $\xi$ is equal to $1/2$, a semi-classical approach gives $\xi = \pi$ [7], nevertheless some measurements presented in [1] for very high $B$ lead to much larger $\xi$.

## 2. Experimental Approach to $\xi$ from the Righi–Leduc Effect and the Kohler Slope

If, in a given transverse magnetic field, the angle $\varphi$ of rotation of the equipotential lines (Hall effect) is equal to the angle of rotation of isothermals (Righi–Leduc effect), we have [19]

$$\tan\varphi = \frac{\rho_{yx}}{\rho_{xx}}. \tag{11}$$

The ratio (11), which is a measure of the Hall angle $\varphi$, is called the Righi–Leduc coefficient.

Experimentally, the ratio (11) has been examined for potassium as a function of $B$ [6]. Because of (9) the result in (11) for $\rho_{yx} = \rho_{yx}^{eff}$, $\rho_{xx} = \rho_{xx}^{eff}$, and large $B$ should be equal to $\xi$. This behaviour is presented in Figure 1 where the experimental data for (11) tend at large $B$ to a quantum-mechanical value of

$$\xi = \frac{1}{2}, \tag{12}$$

obtained in [7].

In numerous experiments referring to the Kohler rule, the ratio

$$\frac{\Delta\rho_{xx}}{\rho_{xx}(0)} = \frac{eB}{mc}\frac{\tau_{el}}{\xi} \tag{13}$$

calculated in [7] is plotted versus the quantity

$$\frac{B}{\rho_{xx}(0)} = \frac{B}{m} e^2 \tau_{el} n_s; \tag{14}$$

see [7] and [8] for (14) and [19–21] for the experimental data. It is easy to show that this plot should lead to a straight line because the expression

$$\frac{\Delta\rho_{xx}}{\rho_{xx}(0)} : \frac{B}{\rho_{xx}(0)} = \frac{\Delta\rho_{xx}}{B} = \frac{1}{ecn_s\xi} \tag{15}$$

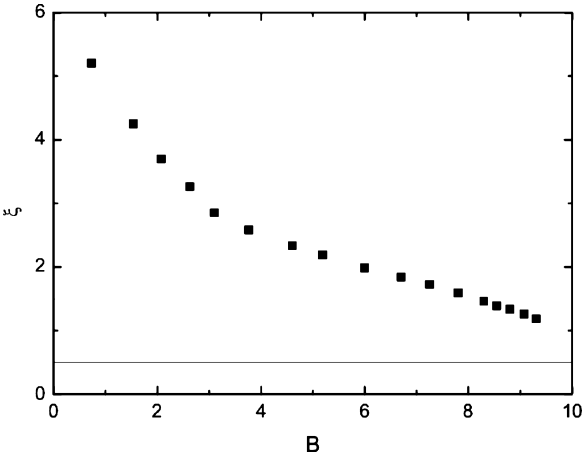


Fig. 1. Experimentally obtained $\xi$ from the Righi–Leduc effect for the metallic potassium, see (10) and [6] (black squares) is compared with a constant $\xi$ calculated in (12). The field strength $B$ is given in Tesla.

is a constant number if $\xi$ is a constant. This constant behaviour of (15) is to a large extent confirmed by the experimental data, for example, for Mg [19]. A universal character of $\xi$, for example its independence of the temperature, is here also confirmed. The experimental measurements on potassium [22] can be also used as an estimate of $\xi$.

## 3. Diagonal Magnetoresistance of Heterostructures

The diagonal magnetoresistance $\rho_{xx}$ of several heterostructures is calculated below in some detail. Various temperatures, carrier concentrations, and chemical compositions are taken into account. A general formula for the change of the resistance in effect of the presence of the magnetic field is

$$\frac{\Delta\rho_{xx}}{\rho_{xx}} = \frac{\rho_{xx}^{eff} - \rho_{xx}}{\rho_{xx}} = \frac{\frac{1}{\tau_{el}} + \frac{1}{\tau(B)} - \frac{1}{\tau_{el}}}{\frac{1}{\tau_{el}}} = \frac{\tau_{el}}{\tau(B)} = \frac{\tau_{el}\Omega_0}{\xi} \tag{16}$$

(cf. here also [7]). The relaxation time $\tau_{el}$ is a parameter entering the diagonal matrix element of the first tensor in (2):

$$\rho_{xx} = \frac{m^{eff}}{n_s e^2 \tau_{el}}, \tag{17}$$

on condition the electron mass $m$ is replaced by an effective mass $m^{\text{eff}}$. Evidently, $\rho_{xx}$ does not vanish at $\|\Delta\rho\| = 0$ or at $B = 0$. For three-dimensional samples the size of $\rho_{xx}$ strongly depends on the temperature $T$, as it is reported by numerous experimental data; see e.g. [23]. For two-dimensional systems an insight into the temperature dependence of resistance is much less elaborated, nevertheless qualitatively it leads to an opposite behaviour than that obtained in three dimensions: the diagonal conductivity of the layers examined for a constant $B$ increases with increase of $T$, at least when this increase begins with very small $T$ [24]. Respectively, a decrease of $T$ produces an increase of resistance [25]. In our calculations, the problem of the dependence of $\tau_{\text{el}}$ and $\rho_{xx}$ on $T$ is avoided since (16) can be transformed with the aid of (17) into

$$\Delta\rho_{xx} = \frac{\tau_{\text{el}}\Omega_0}{\xi}\frac{m^{\text{eff}}}{n_s e^2 \tau_{\text{el}}} = \frac{B}{n_s ec\xi}\frac{m^{\text{eff}}}{m}, \tag{18}$$

so

$$\frac{\Delta\rho_{xx}}{B} = \frac{1}{n_s ec\xi}\frac{m^{\text{eff}}}{m}. \tag{19}$$

Expression (19) is a slope of the resistance change $\Delta\rho_{xx}$ due to the change of $B$, as far as a linear dependence of $\Delta\rho_{xx}$ on $B$ is obtained. In fact, this behaviour is observed experimentally for the considered heterostructures, at least at some specific physical conditions; see example in Figure 2 and Table 2 for detailed data. The ratio between the effective electron mass $m^{\text{eff}}$ due to the band structure and the cyclotron mass $m$ present in $\Omega_0$ in (4) is a necessary correcting factor entering (19): the calculations assume that the cyclotron mass does not differ much from the electron mass $m$. By applying the same units as in (7), the ratio (19) becomes

$$\frac{\Delta\rho_{xx}}{B} = \frac{m}{n_s h}17.6\cdot 10^6 \cdot 25.8\cdot 10^3 \frac{m^{\text{eff}}}{m}\frac{1}{\xi}. \tag{19a}$$

In the next sections, we compare the slopes obtained from (19a) with the experimental data; the quantum-mechanical value $\xi = 1/2$ [7] is put systematically in the calculations.

Table 3 presents the problem of magnetoresistance due to the hole carriers. In principle, the calculations

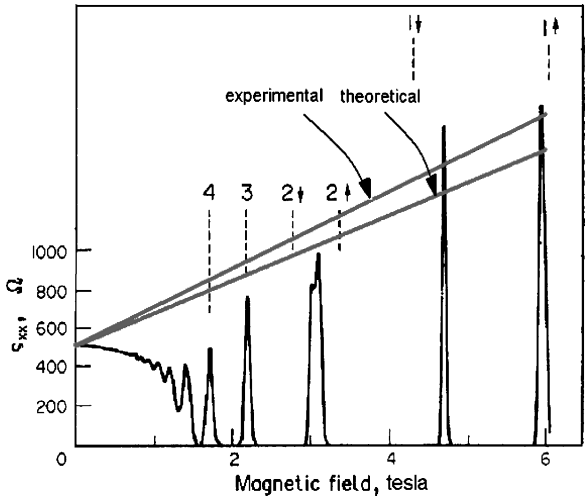


Fig. 2. Experimental and theoretical dependence of the magnetoresistance $\rho_{xx}^{\text{eff}} = \rho_{xx}(B) = \rho_{xx}(B) + \Delta\rho_{xx}$ on the magnetic field induction $B$. The experimental data are taken from [17].

Table 2. Theoretical and experimental slopes of the diagonal magnetoresistance plotted in dependence on $B$. The experimental change of resistance $\Delta\rho_{xx}$ is given in kiloOhm and the induction interval is given in kiloGauss, the carrier concentration $n_s$ is expressed in $10^{11}$ cm$^{-2}$. Theoretical data are obtained from (19a).

| Index | Ref. | $n_s$ | $\frac{m^{\text{eff}}}{m}$ | $\Delta\rho_{xx}^{\text{exp}}$ | $\Delta B^{\text{exp}}$ | $(\frac{\Delta\rho_{xx}}{\Delta B})^{\text{exp}}$ | $(\frac{\Delta\rho_{xx}}{B})^{\text{theor}}$ |
|---|---|---|---|---|---|---|---|
| 1 | [26] | 0.57 | 0.05 | 70 | 110 | 0.63[a] | 0.11 |
| 2 | [27] | 0.61 | 0.05 | 2.7 | 65 | 0.04 | 0.10 |
| 3 | [13] | 0.7 | 0.05 | 0.8 | 95 | 0.008 | 0.09 |
| 4 | [28] | 1.04 | 0.05 | 10 | 60 | 0.17 | 0.06 |
| 5 | [28] | 1.04 | 0.05 | 0.45 | 19 | 0.024 | 0.06 |
| 6 | [2] | 1.21[b] | 0.05 | 4 | 150 | 0.027 | 0.05 |
| 7 | [25] | 1.23 | 0.05 | 20 | 200 | 0.10[c] | 0.05 |
| 8 | [13] | 1.25 | 0.05 | 0.55 | 30 | 0.02 | 0.05 |
| 9 | [29] | 1.26 | 0.55 | 120 | 62 | 1.94 | 0.54 |
| 10 | [30] | 1.48[d] | 0.05 | 8 | 150 | 0.053 | 0.042 |
| 11 | [31] | 1.5 | 0.05 | 2.6 | 80 | 0.03 | 0.04 |
| 12 | [11] | 1.53 | 0.05 | 12.4 | 70 | 0.177 | 0.041 |
| 13 | [13] | 2.1 | 0.05 | 0.6 | 50 | 0.12 | 0.03 |
| 14 | [32] | 2.13 | 0.05 | 24.5 | 235 | 0.10 | 0.029 |
| 15 | [33] | 2.3 | 0.05 | 1 | 55 | 0.018 | 0.027 |
| 16 | [14] | 2.99 | 0.05 | 10.3 | 50 | 0.20 | 0.021 |
| 17 | [34] | 3.0 | 0.05 | 11.1 | 55 | 0.20 | 0.02 |
| 18 | [35] | 3.06 | 0.05 | 3 | 230 | 0.013 | 0.021 |
| 19 | [36] | 3.4 | 0.047 | 1.2 | 80 | 0.015[e] | 0.017 |
| 20 | [17] | 3.7 | 0.05 | 1.2 | 60 | 0.02 | 0.017 |
| 21 | [37] | 6.0 | 0.55 | 0.4 | 35 | 0.011 | 0.10 |
| 22 | [38] | 18 | 0.067 | 0.75 | 75 | 0.01[f] | 0.005 |
| 23 | [40, 41] | 90[g] | 1.4 | 2 | 100 | 0.02 | 0.019 |

[a] $T = 45$ mK
[b] $n_s$ is taken from the Hall resistance data; see Table 1
[c] $T = 4.15$ K
[d] $T = 0.14$ K
[e] $T = 52$ K
[f] $T = 4.2$ K
[g] $n_s$ is obtained from a three-dimensional carrier density

can be based on a reasoning similar to that applied for the electron particles. In particular, this concerns the slopes of the diagonal magnetoresistance plotted versus $B$ which are calculated according to (19a).

A general view on the data given in Tables 2 and 3 indicates that the experimental and theoretical slopes of $\Delta\rho_{xx}/B$ are not so much different quantities. The number of cases when the experimental slopes are larger than the theoretical ones is approximately equal to the number of opposite situations when the theoretical value predominates over its experimental counterpart. The ratios

$$s = \frac{(\Delta\rho_{xx}/B)_{\text{theor}}}{(\Delta\rho_{xx}/\Delta B)_{\text{exp}}} \tag{20}$$

of the theoretical slopes (19a) calculated in Table 2 and Table 3 to the experimental slopes are listed in Table 4 with the chemical composition of the examined heterostructures. The average value of the ratios (20) presented in Table 4 and originating from Table 2 is 1.8, a similar average of the ratios (20) coming from Table 3 is smaller than that obtained from Table 2 and amounts 1.2.

## 4. Discussion

For the carrier concentration which is, say $n_s = N_s/\text{cm}^2$, and the magnetic length $l_B = \left(\frac{\hbar c}{eB}\right)^{1/2}$, (5) for the Hall resistance can be transformed into

$$\rho_{xy}^{\text{eff}} N_s = \frac{B}{ec}\ \text{cm}^2. \tag{21}$$

In the next step, we have

$$1\ \text{cm}^2 = N_d 2\pi l_B^2 = N_d \frac{hc}{eB}. \tag{22}$$

Table 3. Slopes of the theoretical and experimental diagonal magnetoresistance plotted versus the magnetic induction $B$ for the holes. $p_s$ is the hole concentration in $10^{11}$ cm$^{-2}$. The experimental intervals of resistance $\Delta\rho_{xx}$ are given in kiloOhm, intervals of induction $\Delta B$ are in kiloGauss. The theoretical data are calculated from (19a).

| Index | Ref. | $p_s$ | $\frac{m^{\text{eff}}}{m}$ | $\Delta\rho_{xx}^{\text{exp}}$ | $\Delta B^{\text{exp}}$ | $\left(\frac{\Delta\rho_{xx}}{\Delta B}\right)^{\text{exp}}$ | $\left(\frac{\Delta\rho_{xx}}{B}\right)^{\text{theor}}$ |
|---|---|---|---|---|---|---|---|
| 1 | [41] | 0.41 | 0.55 | 350 | 45 | 7.8[a] | 1.5 |
| 2 | [42] | 1.06 | 0.38 | 470 | 145 | 3.2 | 0.45 |
| 3 | [42] | 1.48 | 0.38 | 8 | 80 | 0.1 | 0.32 |
| 4 | [18] | 5.9 | 0.55 | 5.16[b] | 62 | 0.08 | 0.11 |

[a] $T = 22$ mK
[b] $\rho_{xx}$ for $B = 0$ is equal to about 2 kΩ

Table 4. Ratio $s$ of the theoretical slope of magnetoresistance plotted versus $B$ calculated in reference to the experimental slope; see (20). The chemical compositions of the considered heterostructures is also presented.

(a) Ratio $s$ for heterostructures of Table 2:

| Index | $s$ | Composition |
|---|---|---|
| 1 | 0.2 | GaAs/AlGaAs |
| 2 | 2.5 | GaAs/$Al_xGa_{1-x}$As |
| 3 | 11.0 | GaAs/$GaAl_{0.32}$As |
| 4 | 0.4 | GaAs/AlGaAs |
| 5 | 2.5 | GaAs/AlGaAs |
| 6 | 1.9 | GaAs/(Ga, Al)As |
| 7 | 0.5 | GaAs/$Al_{0.3}Ga_{0.7}$As |
| 8 | 2.5 | GaAs/$GaAl_{0.32}$As |
| 9 | 0.3 | $Al_{0.35}Ga_{0.68}$As − Si |
| 10 | 1.3 | GaAs/$Al_xGa_{1-x}$As |
| 11 | 1.5 | GaAs/AlGaAs |
| 12 | 0.2 | GaAs/$Al_{0.33}Ga_{0.67}$As |
| 13 | 0.3 | GaAs/$GaAl_{0.32}$As |
| 14 | 0.3 | GaAs/$Al_{0.3}Ga_{0.7}$As |
| 15 | 1.5 | GaAs/AlGaAs |
| 16 | 0.1 | GaAs/AlGaAs |
| 17 | 0.1 | GaAs/AlGaAs |
| 18 | 1.6 | GaAs/(AlGa)As |
| 19 | 0.9 | $In_xGa_{1-x}As$/InP |
| 20 | 1.1 | GaAs/$Al_xGa_{1-x}$As |
| 21 | 9.1 | Si |
| 22 | 0.5 | AlGaAs/GaAs |
| 23 | 1.0 | $\alpha$-$(BEDT-TTF)_2KHg(SCN)_4$ |

(b) Ratio $s$ for heterostructures of Table 3:

| Index | $s$ | Composition |
|---|---|---|
| 1 | 0.2 | GaAs/AlGaAs − Si |
| 2 | 0.1 | $Al_{0.3}Ga_{0.7}$As |
| 3 | 3.2 | $Al_{0.3}Ga_{0.7}$As |
| 4 | 1.4 | $Si_{0.88}Ge_{0.12}$ |

In effect, (21) becomes

$$\rho_{xy}^{\text{eff}} N_s = \frac{B}{ec} N_d \frac{hc}{eB} = N_d \frac{h}{e^2}, \tag{23}$$

in which $\rho_{xy}^{\text{eff}}$ is expressed in terms of $N_s$, $N_d$, $h$, and $e$.

But a similar situation exists for

$$\Delta\rho_{xx} = \frac{\tau_{\text{el}}\Omega_0}{\xi}\rho_{xx} = \frac{B}{n_s ec}\frac{m^{\text{eff}}}{m}\frac{1}{\xi} \tag{24}$$

which can be transformed into

$$\Delta\rho_{xx} N_s = \frac{B}{ec}\frac{m^{\text{eff}}}{m}\frac{1}{\xi}\ \text{cm}^2 = \frac{B}{ec}\frac{m^{\text{eff}}}{m}\frac{1}{\xi} N_d \frac{hc}{eB} = N_d \frac{h}{e^2}\frac{m^{\text{eff}}}{m\xi}. \tag{25}$$

Here the quanta of $h/e^2$ in (23) are replaced by the new ones which are equal to

$$\frac{h}{e^2}\frac{m^{\mathrm{eff}}}{m\xi}. \tag{26}$$

It seems that the size of the factor $m^{\mathrm{eff}}/m\xi$ entering (26) can be decisive for the behaviour of magnetoresistance in dependence on the sample temperature. For $m^{\mathrm{eff}}/m\xi \ll 1$, the resistance quanta (26) become much smaller than $h/e^2$ and are made more suitable for the temperature excitement. On the other hand, in case of $m^{\mathrm{eff}}/m\xi > 1$ which is a situation met in $\alpha$-$(\mathrm{BEDT-TTF})_2\mathrm{KHg(SCN)}_4$ [39] we have the expression in (26) larger than $h/e^2$. Simultaneously, an experimental behaviour observed in the absence of the magnetic field indicates a systematic decrease of the diagonal resistance with decrease of the temperature [40], similar to that observed for the three-dimensional metals [23].

Preliminary experimental and theoretical data for the constant $\xi$ were discussed in [43, 44].

Another experimental source of $\xi$ for planar structures can be an examination of the width $2\Gamma$ of the Landau levels considered as a function of $B$. This width is coupled with the relaxation time $\tau(B)$ by the well-known relation

$$2\Gamma = \frac{\hbar}{\tau(B)} = \frac{\hbar}{\xi}\Omega_0, \tag{27}$$

where the second step is dictated by (3). In consequence of a constant behaviour of $\xi$, the width $2\Gamma$ becomes proportional to $B$; see (4). This property has been already derived on an experimental basis [45].


[1] A. H. MacDonald, Quantum Hall Effect: a Perspective, Kluwer Academic, Milano 1989.
[2] J. Singleton, Band Theory and Electronic Properties of Solids, Oxford University Press, Oxford 2001.
[3] I. M. Lifshitz, M. Ya. Azbel, and M. I. Kaganov, Zh. Eksper. i Teor. Fiz. **30**, 220 (1955); **31**, 63 (1956) [Sov. Phys. JETP **3**, 143 (1956); **4**, 41 (1957)].
[4] P. A. Penz and R. Bowers, Phys. Rev. **172**, 991 (1968).
[5] H. Taub, R. L. Schmidt, B. W. Maxfield, and R. Bowers, Phys. Rev. B **4**, 1134 (1971).
[6] P. J. Tausch and R. S. Newrock, Phys. Rev. B **16**, 5381 (1977).
[7] S. Olszewski and M. Gluzinski, Z. Naturforsch. **66a**, 311 (2011).
[8] C. Kittel, Quantum Theory of Solids, 2nd ed. Wiley, New York 1987.
[9] S. Olszewski, M. Pietrachowicz, and M. Baszczak, Phys. Stat. Sol. (b) **241**, 3572 (2004).
[10] D. C. Tsui, Rev. Mod. Phys. **71**, 891 (1999).
[11] C. T. Liang, C. G. Smith, M. Y. Simmons, and D. A. Ritchie, Phys. Rev. B **64**, 233319 (2001).
[12] M. Heilblum and A. Stern, Phys. World **13**, 37 (2000).
[13] R. G. Clark, R. J. Nicholas, A. Usher, C. T. Foxon, and J. J. Harris, Surf. Sci. **170**, 141 (1986).
[14] J. P. Eisenstein and H. L. Strmer, Science **248**, 1510 (1990).
[15] K. Vyborny, L. Smrcka, and R. A. Deutschmann, Phys. Rev. B **66**, 205318 (2002).
[16] S. Valfells, J. S. Brooks, Z. Wang, S. Takasaki, J. Yamada, H. Anzai, and M. Tokumoto, Phys. Rev. B **54**, 16413 (1996).
[17] G. Ebert, K. von Klitzing, C. Probst, and K. Ploog, Solid State Commun. **44**, 95 (1982).
[18] P. T. Coleridge, A. S. Sachrajda, H. Lafontaine, and Y. Feng, Phys. Rev. B **54**, 14518 (1996).
[19] J.-P. Jan, in: Solid State Physics Vol. 5 (Eds. F. Seitz, D. Turnbull), Academic, New York 1957.
[20] P. Kapitza, Proc. Roy. Soc. A **123**, 292 (1929).
[21] M. Kohler, Ann. Phys. **32**, 211 (1938).
[22] H. Taub, Phys. Cond. Matter **19**, 107 (1975).
[23] Landoldt-Bornstein, Zahlenwerte und Funktionen Vol. 2, Part 6, Springer, Berlin 1959.
[24] M. A. Paalanen, D. C. Tsui, and A. C. Gossard, Phys. Rev. B **25**, 5566 (1982).
[25] D. C. Tsui, H. L. Stormer, and A. C. Gossard, Phys. Rev. Lett. **48**, 1559 (1982).
[26] V. J. Goldman, J. K. Wang, B. Su, and M. Shayegan, Phys. Rev. Lett. **70**, 647 (1993).
[27] T. Sajoto, Y. P. Li, L. W. Engel, D. C. Tsui, and M. Shayegan, Phys. Rev. Lett. **70**, 2321 (1993).
[28] J. P. Eisenstein, G. S. Boebinger, L. N. Pfeiffer, K. W. West, and H. Song, Phys. Rev. Lett. **68**, 1383 (1992).
[29] H. C. Manoharan, Y. W. Suen, M. P. Santos, and M. Shayegan, Phys. Rev. Lett. **77**, 1813 (1996).
[30] D. C. Tsui, H. L. Stormer, and J. C. M. Hwang, Phys. Rev. B **28**, 2274 (1983).
[31] G. S. Boebinger and A. M. Chang, Phys. Rev. B **32**, 4268 (1985).
[32] A. M. Chang, P. Berglund, D. C. Tsui, H. L. Stormer, and J. C. M. Hwang, Phys. Rev. Lett. **53**, 997 (1984).
[33] J. P. Eisenstein, H. L. Stormer, L. Pfeiffer, and K. W. West, Phys. Rev. Lett. **62**, 1540 (1989).

[34] R. Willett, J. P. Eisenstein, H. L. Stormer, D. C. Tsui, A. C. Gossard, and J. H. English, Phys. Rev. Lett. **59**, 1776 (1987).
[35] H. L. Stormer, D. C. Tsui, A. C. Gossard, and J. C. M. Hwang, Physica **117/118**, 688 (1983).
[36] H. P. Wei, D. C. Tsui, and A. M. M. Pruisken, Phys. Rev. B **33**, 1488 (1985).
[37] G. S. Boebinger, H. W. Jiang, L. N. Pfeiffer, and K. W. West, Phys. Rev. Lett. **64**, 1793 (1990).
[38] A. A. Gorbatsevich, V. V. Kapaev, Y. V. Kopayev, I. V. Kucherenko, O. E. Omel'yanovskii, and V. I. Tsebro, J. Exp. Theor. Phys. **93**, 833 (2001).
[39] C. E. Campos, J. S. Brooks, P. J. M. van Bentum, J. A. A. J. Perenboom, S. J. Klepper, P. S. Sandhu, S. Valfells, Y. Tanaka, T. Kinoshita, N. Kinoshita, M. Tokumoto, and H. Anzai, Phys. Rev. B **52**, R7014 (1995).
[40] T. Sasaki, S. Endo, and N. Toyota, Phys. Rev. B **48**, 1928 (1993).
[41] M. B. Santos, Y. W. Suen, M. Shayegan, Y. P. Li, L. W. Engel, and D. C. Tsui, Phys. Rev. Lett. **68**, 1188 (1992).
[42] H. C. Manoharan and M. Shayegan, Phys. Rev. B **50**, 17662 (1994).
[43] S. Olszewski and R. Kozak, Phys. Rev. B **67**, 224434 (2003).
[44] S. Olszewski and T. Rolinski, Physica B **403**, 2043 (2008).
[45] F. M. Peeters and P. Vasilopoulos, Phys. Rev. B **47**, 1466 (1993).